ISSN 2250-3153

Bifurcation Analysis and Chaos in Electronic Genetic Toggle Switch

Félix Mateus[1, 2], Feng Liu[1]

[1]School of Automation, China University of Geosciences, Wuhan, 430074, P.R. China
[2]Songo Higher Education Polytechnic Institute, Tete, 3204, Republic of Mozambique
Full information of the authors is available at the end of the article.

DOI: 10.29322/IJSRP.9.02.2019.p8619
http://dx.doi.org/10.29322/IJSRP.9.02.2019.p8619

Abstract: In this paper, an electronic (Transistor MOSFET) genetic toggle switch is discretized by the Euler method. The proposed model is discussed by using ordinary differential equations that describe the system behaviour. The stability has been analysed using Jacobian matrix, theorems, and lemmas that illustrate its stability. Two units of MOSFET transistors compose the proposed circuit model, which acts as two genes repressing each other. Different behavior has been analysed such as bifurcation and chaos, based on the numerical simulations that illustrate the theoretical results.

Key words: Genetic Toggle Switch; Bifurcation; Chaos; Electronic Toggle Switch.

1. Introduction

Gardner et al. investigated a genetic toggle switch model and presented the construction of engineered gene-regulatory network in bacterium Escherichia coli that preformed as a genetic toggle switch [1]. The genetic toggle switch is a simple network of two repressor gene, where each of the repressor proteins binds to the promoter of the other one [2], (see fig.1). It means, when a repressor dominates, the system remains at the same state unless an exogenous inducer (e.g., a protein or a temperature shift) effect changes it, by degrading artificially one of the repressors, so another one shift its previous state. Simply, the switches allows genes to be ON in one tissue but OFF in another. After a jump between states, which is a variation of the protein concentration, the system keeps the protein level. It can be compared to Reset-set latch, which memorize its current state indefinitely until an external inducer acts again.

Previous study in electronic genetic networks (EGNs) used hybrid digital-analog system circuits based on AND, OR functions by using complementary metal oxide semiconductor CMOS chips and RC circuits to model the logical control of the increase and decay of protein concentration in the system [3]. The model from which we proposed to investigate the electronic genetic toggle switch is derived from a reduction of an electronic circuit of the repressilator based on the N-channel metal-oxide-semiconductor field-effect transistor (MOSFET) [4]. The repressilator is comprised of three basic units that corresponds to the three genes, the proposed model have only two basic units, each one consisting of a RC circuit and a MOSFET transistor (T1 and T2 respectively). In order to perform the bistability we assume that the voltage applied on T1 is high. In such way that it is applied at the gate of the T2, it will inhibits the T2, whose output voltage is switched off. Simply, if the voltage applied to the gate exceeds a certain threshold voltage the transistor switches off its output, leading to an output voltage close to zero, (the transistor has very low output impedance) [5].

Jing in [6] described a genetic toggle switch model and presented the stability of the fixed points and bifurcations behaviours, applying the forward Euler scheme to discrete the model by bifurcation theory of continuous and discrete systems. Where chaotic behaviour was one of the behaviour analysed in the model. Chaos oscillations characterized by sensitivity to initial conditions typically occur in dynamical systems with more than two variables, described by couple ordinary differential equations ODEs. A well-known property of chaotic system is that any initially tiny error will be exponentially amplified by chaotic dynamics, so that a pair of highly similar initial conditions will rapidly be de-correlated, making the behaviour of the system appear stochastic [7].

In this paper, our aim is to study the stability as well as the analysis of chaos behaviour in the proposed circuit based on the Euler's method [8].

The paper is organized as follows. In Section 2, we present the proposed system and we recall the equations of the genetic toggle switch model and illustrate the main dynamical properties of the systems. In Section 3, we study the stability of the system by applying the Euler's method to discretize the main equation that describe the genetic toggle switch using electronic components. In the section 4, theorems and lemmas are used to prove the stability according to the required terms and condition. In the section 5, truncated Taylor series centered on the steady state point of interest to linearize the model is presented. In the section 6, bifurcation diagrams are analysed in different conditions by manipulating the parameters. Then finally in the section 6, we bring a discussion about the obtained results.

2. System Description

Figure 1 illustrates the interations of a genetic toggle switch, where in fig. 1 a) the arrows represent promoters (P_L and *Ptrc* 2) , the bistabilty is achieved by repressing the two genes (*cl-ts* and *lacI*). In fig. 1 b) an electronic approach of a genetic toggle switch consisting on two MOSFET transistors which replace the previous model.

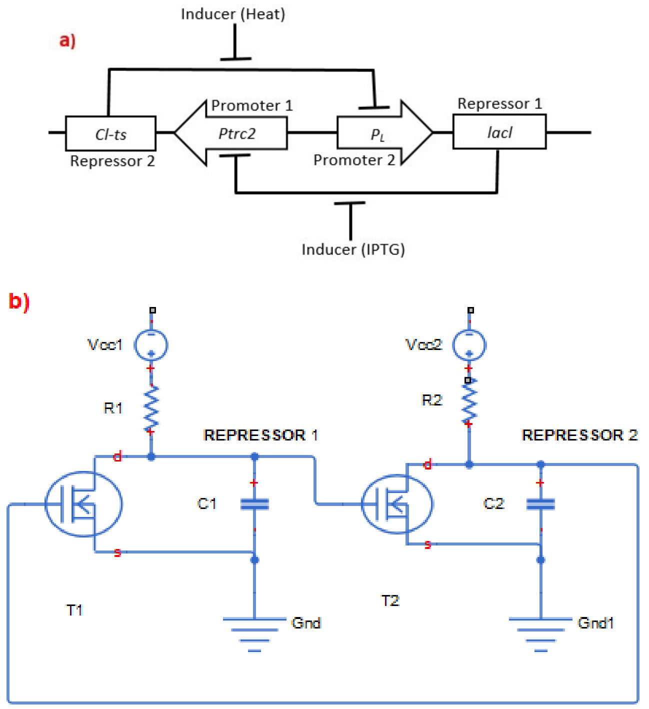

Fig. 1 a) Schematic representation of a bistable genetic network toggle switch. The repressor genes are mutually connected by negative feedback. Promoters of each gene are repressed by protein transcripted from the previous gene. **b)** Electronic circuits of the genetic toggle switch based on MOSFET transistors. The output of each transistors (T_1 and T_2) corresponds to the level of two repressors protein. V_1 and V_2 correspond to the voltage at terminals of C_1 and C_2 respectively.

The equations (2.1) describe the circuit 1.b), which is derived from a biochemical rate equation formulation of gene expression [1]

$$\frac{dv_1}{dt} = \frac{-V_1 + V_{cc}[f(V_2)]}{R_1C_1}$$
$$\frac{dv_2}{dt} = \frac{-V_2 + V_{cc}[f(V_1)]}{R_2C_2} \tag{2.1}$$

where $V_{cc} = V_{cc1} = V_{cc2}$ is the voltage source and the function $f(x)$ depends on the transistor parameters and should be sigmoidal shape, as it represents a switch (for small changes in signal the response at a certain threshold switches from null to high, from OFF to ON, from 0 to 1) and can be written as

$$f(x) = \frac{\alpha}{1+\beta x^{\mu}} \tag{2.2}$$

where α, β and μ are the MOSFET transistor parameters. Equation (2.2) corresponds to the Michaelis-Menten equation of growth of μ as the Hill coefficient.

3. Stability analysis

To analyze the system accurately let substitute (2.2) in (2.1) thus

$$\frac{dv_1}{dt} = \frac{V_{cc}}{R_1C_1}\cdot\frac{\alpha}{\left(1+\beta v_2^{\gamma_1}\right)} - v_1$$
$$\frac{dv_2}{dt} = \frac{V_{cc}}{R_2C_2}\cdot\frac{\alpha}{\left(1+\beta v_1^{\gamma_2}\right)} - v_2 \tag{3.1}$$

Applying Euler method the discretization (3.1) can be derived, in order to maintain the property of convergence to the equilibrium, regardless of the step size. Hence from (3.1) the equations (3.2) are obtained

$$\frac{V_{cc}\cdot\alpha}{R_1C_1} = a \qquad \frac{V_{cc}\cdot\alpha}{R_2C_2} = b \tag{3.2}$$

Let $t_{in} = n\delta$, where δ is step size. Applying Euler's method we obtain

$$v_{1(n+1)} = \frac{a\delta}{1+\beta(v_{2n})^{\gamma_1}} + (1-\delta)v_{1n}$$
$$v_{2(n+2)} = \frac{b\delta}{1+\beta(v_{1n})^{\gamma_2}} + (1-\delta)v_{2n} \tag{3.3}$$

Rewriting the parameters in (3.2) by $a\delta \to A$, $b\delta \to B$, $1-\delta \to \rho$ the equations (3.4), which are discrete dynamical system.

$$v_{1(n+1)} = \frac{A}{1+\beta\cdot(v_{2n})^{\gamma_1}} + \rho v_{1n}$$
$$v_{2(n+2)} = \frac{B}{1+\beta\cdot(v_{1n})^{\gamma_2}} + \rho v_{2n} \tag{3.4}$$

In this section, we will study the dynamics behavior of the system (3.4) such as stability and the bifurcation phenomenon. We will use some theorem and lemmas to illustrate existence conditions of unique positive root, local asymptotic stability and global asymptotic behavior of discrete dynamical system (3.4).

4. Results

Theorem 4.1 Taking $\rho < 1$. Therefore, every solutions in the system (3.4) is bounded in space and persists.

Proof: Let $\{(v_{1n}, v_{2n})\}$ be any arbitrary positive solution of (3.4), then it can be written has

$$v_{1(n+1)} \le A + \rho v_{1n}, \quad v_{2(n+1)} \le B + \rho v_{2n}$$

Where for $n = 0,1,2\cdots$. In addition, substituting the terms, considering the following system of equations:

$$v_{1(n+1)} = A + \rho v_{1(n)}, \quad v_{2(n+1)} = A + \rho v_{2(n)}$$

The solution for the initial conditions of the linear system is given by

$$v_{1(n)} = \frac{A(1-\rho^n)}{1-\rho} + C^n v_{1(0)}, v_{2(n)} = \frac{B(1-\rho^n)}{1-\rho} + \rho^n v_{2(0)}$$

$n = 0$, then the equation is written as follows

$$v_{1(n)} \le \frac{A}{1-\rho} + v_{1(0)}, v_{2(n)} \le \frac{B}{1-\rho} + v_{2(0)}$$

Rewriting (3.4), observing the initial conditions $v_{1(0)} = x_0, v_{2(0)} = y_0$ follows that

$$v_{1(n+1)} \ge \frac{A}{1+\beta(v_{2n})^{\gamma}} \ge \frac{A}{1+\beta\cdot\left(\frac{B}{1-\rho}\right)^{\gamma_1}} = k$$

$$v_{2(n+2)} \ge \frac{B}{1+\beta(v_{1n})^{\gamma}} \ge \frac{B}{1+\beta\cdot\left(\frac{A}{1-\rho}\right)^{\gamma_2}} = k^*$$

Then

$$k \le v_{1(n)} \le \frac{A}{\beta\cdot(1-\rho)}, k^* \le v_{2(n)} \le \frac{B}{\beta\cdot(1-\rho)}$$

For all $n = 1,2\cdots$. The proof is complete.

The set from the previous proof

$\left[k, \frac{A}{\beta(1-\rho)}\right], \left[k^*, \frac{B}{\beta(1-\rho)}\right]$ is an invariant set considering $\rho < 1$ and β selected from an MOSFET transistor parameters, taking it from the initial conditions in system (3.4).

Theorem 4.2: Taking $\rho < 1$, therefore (3.4) has unique positive equilibrium point

$(\overline{v}_{1n}, \overline{v}_{2n}) \in \left[K, \frac{A}{\beta(1-\rho)}\right], \left[K^*, \frac{B}{\beta(1-\rho)}\right]$, if the following condition is verified:

$$k < \frac{B}{\beta(1-\rho)\left[1+\left(f(v_1)\right)^{\gamma_1}\right]}$$

Proof: Let's consider the system (4.1),

$$\begin{aligned} v_1 &= \frac{A}{1+\beta(v_2)^{\gamma_1}} + \rho v_1 \\ v_2 &= \frac{B}{1+\beta(v_1)^{\gamma_2}} + \rho v_2 \end{aligned} \tag{4.2}$$

assuming the set

$$(v_1, v_2) \in \left[K, \frac{A}{\beta(1-\rho)}\right], \left[K^*, \frac{B}{\beta(1-\rho)}\right]$$

we write the function

$$G(v_1) = \frac{A}{\beta(1-\rho)[1+f(v_1)^{\gamma_1}]} - v_1$$

where,

$$f(v_1) = \frac{B}{\beta(1-\rho)(1+v_1^{\gamma_2})}$$

Then, the first ODEs are written as follow

$$y = \left[f(x)\right]^n \to y' = n\cdot\left[f(x)\right]^{n-1}\cdot f'(x)$$

$$G'(v_1) = -\frac{A\gamma f(v_1)^{\gamma_1-1}\cdot f'(v_1)}{\beta(1-\rho)\left(1+f(v_1)^{\gamma_1}\right)^2} - 1$$

and

$$f'(v_1) = -\frac{B\gamma v_1^{\gamma_2-1}}{\beta(1-\rho)(1+v_1^{\gamma_2})^2}$$

Therefore, $k = v_1$. End let w be a solution when $G(v_1) = 0$, then $w = \frac{A}{\beta(1-\rho)\left(1+f(w)^{\gamma_1}\right)}$.Thus,

$$G'(w)=\frac{A\gamma_1\gamma_2 w^{\gamma_2-1}\left(\frac{B}{\beta(1-\rho)(1+w^{\gamma})}\right)^{\gamma_1+1}}{B\left(1+\left(\frac{B}{\beta(1-\rho)(1+w^{\gamma})}\right)^{\gamma_1}\right)^2}-1$$

$$=\frac{\gamma_1\gamma_2\left(\frac{A}{\beta(1+\rho)}\right)^{\gamma_2}[A-\beta(1-\rho)\cdot K]}{A\left(1+K^{\gamma_2}\right)}-1<0$$

This proofs the theorem 3.2.

Lemma 4.1 Form [9], in discrete dynamical system of the form $X_{(n+1)}=G_{(x_n)}$, for $n=0,1,...$ and $\bar{x}$ is an equilibrium point of G. Then, the fixed point is locally asymptotically stable if all the eigenvalues of the Jacobian matrix G_J around the fixed point are less than one in absolute value $|\lambda|<1$ and is unstable if there exists at least one of the eigenvalues of G_J with absolute value greater than one [10].

Lemma 4.2 Consider the canonical form of the square function [10].

$$\lambda^2+a_1\lambda+a_2=0, \qquad (4.3)$$

Where a_1 and a_2 are real values. Then, the necessary and sufficient condition for the solution of the equation (4.3), around the numbers $|\lambda|<1$ is $|a_1|<1$ and $a_2<2$.

Theorem 4.3 If the condition

$$2\rho+\rho^2+\frac{\gamma_1\gamma_2\beta A^{\gamma_2}B^{\gamma_1}}{\beta(1-\rho)^{\gamma_1+\gamma_2-2}}<1$$

holds, then the unique positive equilibrium $\left(\bar{v}_1,\bar{v}_2\right)$ of the system (3.4) is locally asymptotically stable.

The characteristic equation of the linearization of the system around the fixed point $\left(\bar{v}_1,\bar{v}_2\right)$ is given by

$$G_J\left(\bar{v}_1,\bar{v}_2\right)=\begin{bmatrix}\rho & -\frac{A\beta\gamma_1\bar{v}_2^{\gamma_1-1}}{1+\beta\cdot\bar{v}_2^{\gamma_1}}\\ -\frac{B\beta\gamma_2\bar{v}_1^{\gamma_2-1}}{1+\beta\cdot\bar{v}_1^{\gamma_2}} & \rho\end{bmatrix}$$

From [11], the characteristic equation

$$\det(A_J-\lambda I)=0, \qquad (4.4)$$

and the characteristic polynomial

$$\lambda^2-\left(traceJ\right)\lambda+\left(\det J\right)=0 \qquad (4.5)$$

of $G_J\left(\bar{v}_1,\bar{v}_2\right)$ is written as

$$\lambda^2-2\rho\lambda+\rho^2-\frac{AB\beta^2\gamma_1\gamma_2\bar{v}_1^{\gamma_2-1}\bar{v}_2^{\gamma_1-1}}{\left(1+\beta\cdot\bar{v}_1^{\gamma_2}\right)^2\left(1+\beta\cdot\bar{v}_2^{\gamma_1}\right)^2}=0 \qquad (4.6)$$

Considering $|\lambda|=1$, and the equations (3.5)

$$\bar{v}_1=\frac{A}{1+\beta(\bar{v}_2)^{\gamma_1}},\bar{v}_2=\frac{B}{1+\beta(\bar{v}_1)^{\gamma_2}} \qquad (4.7)$$

The equation (3.4) can be written as follow

$$2\rho+\rho^2+\frac{\gamma_1\gamma_2\beta A^{\gamma_2}B^{\gamma_1}}{\beta(1-\rho)^{\gamma_1+\gamma_2-2}}<1$$

This equation is a proof and the necessary condition of the theorem (3.3).

The stability using 3.3, it follow $traceJ=2\rho$

$$\det J=\rho^2-\rho^2\frac{AB\beta^2\gamma_1\gamma_2\bar{v}_1^{\gamma_2-1}\bar{v}_2^{\gamma_1-1}}{\left(1+\beta\cdot\bar{v}_1^{\gamma_2}\right)^2\left(1+\beta\cdot\bar{v}_2^{\gamma_1}\right)^2}$$

$=\rho^2-\rho^2 z$, where $z=\frac{AB\beta^2\gamma_1\gamma_2\bar{v}_1^{\gamma_2-1}\bar{v}_2^{\gamma_1-1}}{\left(1+\beta\cdot\bar{v}_1^{\gamma_2}\right)^2\left(1+\beta\cdot\bar{v}_2^{\gamma_1}\right)^2}$

and then by

$$(trJ)^2-4\left(\det J\right)=\frac{AB\beta^2\gamma_1\gamma_2\bar{v}_1^{\gamma_2-1}\bar{v}_2^{\gamma_1-1}}{\left(1+\beta\cdot\bar{v}_1^{\gamma_2}\right)^2\left(1+\beta\cdot\bar{v}_2^{\gamma_1}\right)^2}>0$$

We obtain that the eigenvalues of the fixed point of map (2.6) using the equation

$\lambda_{1,2}=\frac{traceJ\pm\sqrt{\left(traceJ\right)^2-4\left(\det J\right)}}{2}$, are all real.

We can analyse the stability of fixed points as following

Theorem 4.4

i. One eigenvalue of (3.3) is positive if $z=1$; one is negative if $z=\left(1-\dfrac{2}{\rho}\right)^2$.

ii. The fixed point $\left(\overline{v}_1,\overline{v}_2\right)$ of map (2.6) is stable if $0<z<1$, and $0<\rho<\rho'$ taking $\rho'=\dfrac{2-2\sqrt{z}}{1-z}$.

Ingalls in [12], the stability is analyzed using the fundamental equations of the genetic toggle switch, and applying the same analogy from (3.1) the fig. 2 is obtained when the parameters are set as follow $\alpha=5$, $\beta=\frac{1}{2}$ $\gamma_1=\gamma_2=\gamma=2$ and other parameters are in the Table I.

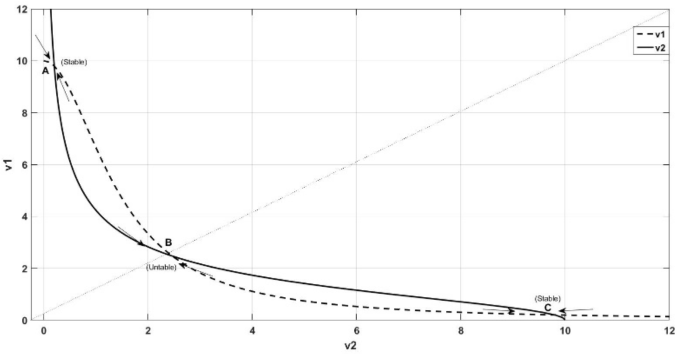

Fig. 2. Genetic toggle switch, by analysing the direction of the vector field in the proximity of the equilibrium, one can deduce their stability. The points **A** and **C** the arrows shows the equilibrium point when the equations (3.1) are set to zero (Nullclines), the bistability occurs, and on point **B** the dashed 45^0 line divides the plane into the two regions of attraction of the stable equilibrium points.

The stead state of the nullclines plotted in the fig.2 must be evaluated separately in order to analyze the stability. And knowing that the model is non-linear. To compute the eigenvalues of our model matrix, we have to calculate the intersections of the nullclines, which for the three stead states will give us the initial point to the intersection, where for our model considering initial conditions $(0,0)$ we get $\begin{bmatrix}3,5032\\3,5032\end{bmatrix}$ as our relevant initial point, which will be discussed in the next section.

5. Linearization of the model

To linearize (3.1) we will use a truncated Taylor series cantered on the steady state point of interest

$$G\left(v_1,v_2\right)\cong G(v_{1(0)},v_{2(0)})+(v_1,v_{1(0)})\left.\frac{\partial g}{\partial v_1}\right|_{v_{1(0)},v_{2(0)}} +(v_2,v_{2(0)})\left.\frac{\partial g}{\partial v_2}\right|_{v_{1(0)},v_{2(0)}} \tag{5.1}$$

We first, calculate the partial differential equation of (3.1) with respect to v_1, it follow

$$G\left(v_1,v_2\right)=\frac{dv_1}{dt}=\frac{V_{cc}}{R_1C_1}\cdot\frac{\alpha}{\left(1+\beta v_2^{\gamma_1}\right)}-v_1$$

$$\frac{\partial g}{\partial v_1}=-1 \qquad \left.\frac{\partial g}{\partial v_1}\right|_{v_{1(0)},v_{2(0)}}=-1$$

Then, the partial differential equation with respect to v_2

$$\left.\frac{\partial g}{\partial v_2}\right|_{v_{1(0)},v_{2(0)}}=-\frac{V_{cc}}{R_1C_1}\cdot\frac{\alpha\beta\gamma_1 v_2^{\gamma_1-1}}{\left(1+\beta v_2^{\gamma_1}\right)^2}$$

$$\left.\frac{\partial g}{\partial v_2}\right|_{v_{1(0)},v_{2(0)}}=-\frac{5\times2\times\frac{1}{2}\times(3,5032)^{2-1}}{10^3\times(0.1\times10^{-3})\times[1+(\frac{1}{2}.3,5032)^2]^2}=-9,981$$

$$\frac{dv_1}{dt}=-1\cdot(v_1-v_{1(0)})-9,981\cdot(v_2-v_{2(0)})$$

By the symmetry, we get

$$\frac{dv_2}{dt}=-9,981\cdot(v_1-v_{1(0)})-1\cdot(v_2-v_{2(0)})$$

The variable transformation as $\tilde{v}_1=v_1-v_{1(0)}$ and $\tilde{v}_2=v_2-v_{2(0)}$.

Then, we write

$$\frac{d\tilde{v}_1}{dt}=-1\cdot\tilde{v}_1-9,981\cdot\tilde{v}_2$$

$$\frac{d\tilde{v}_2}{dt}=-9,981\cdot\tilde{v}_1-1\cdot\tilde{v}_2$$

Writing the model matrix

$$\frac{d\tilde{v}_1}{dt}=J\cdot\tilde{v}_1 \tag{5.2}$$

$$J = \begin{pmatrix} -1 & -9,981 \\ -9,981 & -1 \end{pmatrix}$$

Let us recall, this is an approximation of our model around the point $(v_1 = v_{1(0)})$ and $(v_2 = v_{2(0)})$, and it can be around $(\tilde{v}_1 = 0, \tilde{v}_2 = 0)$. From the Jacob matrix, we can investigate if our first steady state point is stable. Computing the eigenvalues, we get $(\lambda_1 = -10.981, \lambda_2 = 8.981)$. From the eigenvalues clearly, we see that this equilibrium is not stable.

As we keep evaluating the Jacobian matrix and its eigenvalues for the other stationary (second and third) points.

For our system, assuming that $\gamma_1 = \gamma_2 = \gamma$, we can write

$$J = \left. \begin{pmatrix} -1 & -\frac{V_{cc}}{R_1 C_1} \cdot \frac{\alpha\beta\gamma v_2^{\gamma-1}}{\left(1+\beta v_2^{\gamma}\right)^2} \\ -\frac{V_{cc}}{R_2 C_2} \cdot \frac{\alpha\beta\gamma v_1^{\gamma_1-1}}{\left(1+\beta v_1^{\gamma}\right)^2} & -1 \end{pmatrix} \right|_{v_{1(0)}, v_{2(0)}}$$

$$J = \begin{pmatrix} -1 & -0.255 \\ -1.745 & -1 \end{pmatrix}$$

We get the following eigenvalues,

$$(\lambda_1 = -0.3333, \lambda_2 = -1.6667)$$

Which shows that the second and the third (by symmetry) stationary points are stable (see fig.2).

6. Bifurcation

Let rewrite the system (2.1) as a function of v_2 showed in (6.1)

$$G(v_2) = \left(\frac{V_{cc}\alpha}{R_1 C_1 (1+\beta v_2^{\gamma_1})}\right)^{\gamma_2} - \left(\frac{V_{cc}\alpha}{R_2 C_2 v_2} - 1\right)^{1/\beta} \quad (6.1)$$

TABLE I. NUMERICAL CONSTANT VALUES OF THE ELECTRONIC COMPONENTS USED IN THE SIMULATION

Symbol	Parameter	Value	Units
R_i	Resistance	1.0	$k\Omega$
C_i	Capacitor	0.1	mF
V_{cc}	Voltage Source	5.0	V
$MOSFET\ T_i$	Transistor 2N7000	x	x

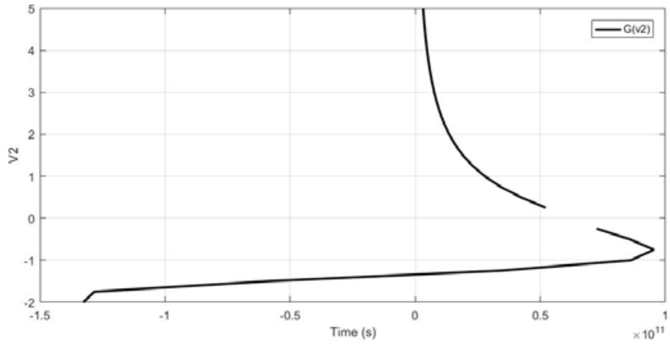

Fig. 3. Bifurcation diagram of map (5.1) $\alpha = 5$, $\beta = 1/2$ $\gamma_1 = 1.2$, $\gamma_2 = 2$.

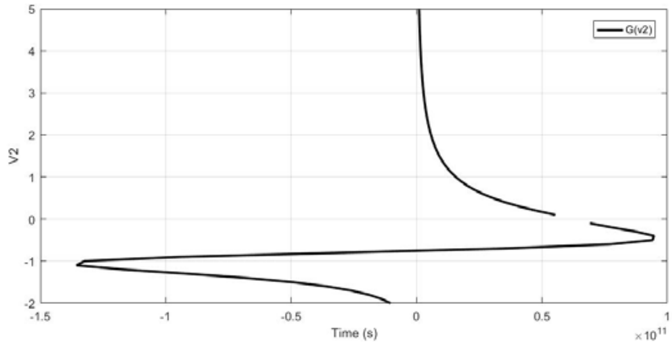

Fig. 4. Bifurcation diagram of map (5.1) $\alpha = 5$, $\beta = 1$ $\gamma_1 = 1.2$, $\gamma_2 = 2$.

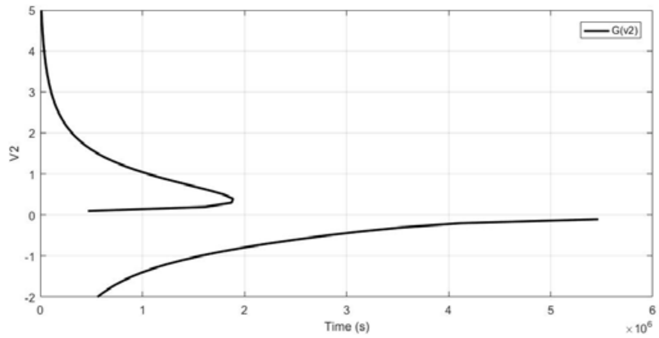

Fig. 5. Bifurcation diagram of map (5.1) $\alpha = 5$, $\beta = 1$ $\gamma_1 = 2$, $\gamma_2 = 1.2$.

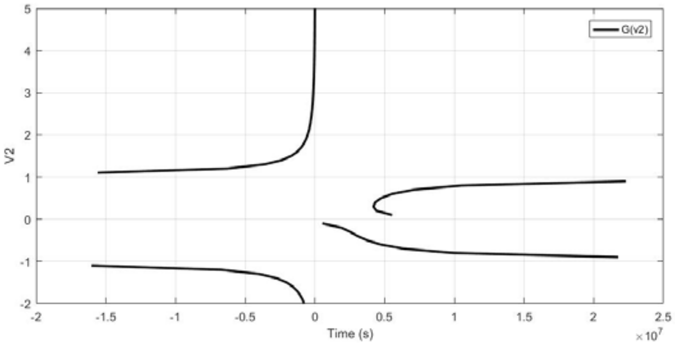

Fig. 5. Bifurcation diagram of map (5.1) $\alpha = 5$, $\beta = 1$ $\gamma_1 = 2$, $\gamma_2 = 2$.

7. Discussion

To analyse the simulation results we should know that the parameters are selected according to what we are seeking to get. Also is required to think of this as a biological control system that tries to keep two concentrations equal. The rate at which the controller perform is $1/\beta$ [12].

The diagram in the fig. 2, was obtained by setting the following parameters $\alpha = 5$, $\beta = 1/2$ $\gamma_1 = 1.2$, $\gamma_2 = 2$ on map (5.1). Which shows the region of bistability [13]. In the fig. 3 by varying the parameter β we can see that the rate increase and the shift time is also increased. In the fig. 5 shows the bifurcation diagram clearly more complex dynamical than fig 4, where according to the bifurcation phenomena leads to chaos, this chaotic behavior brings interior crisis. So the selection of β and γ should be very wise.

8. Conclusion

In this paper, we have investigated the behaviors of the genetic toggle switch model as a dynamical system, and found interesting behaviours patterns in the numerical simulations by varying the circuit parameters. The analyses and results are very important for understanding nature gene network applying electronic circuits to develop novel ways that emitted the living organism. It further shows how genetic toggle switch perform an important role in synthetic genetic networks.

The circuit behavior was analysed and verified by comparing bifurcation diagrams according to the simulations.

References

[1] Gardner T S, Cantor C R, Collins J J. Construction of a genetic toggle switch in Escherichia coli. [J]. Nature, 2000, 403(6767):339.

[2] Wagemakers A, Buldú J M, Garcíao Jalvo J, et al. Synchronization of electronic genetic networks [J]. Chaos An Interdisciplinary Journal of Nonlinear Science, 2006, 16(1):318-356.

[3] Mason J, Linsay P S, Collins J J, et al. Evolving complex dynamics in electronic models of genetic networks [J]. Chaos, 2004, 14(3):707-715.

[4] Guang-Bi L I, Meng L Z, Liu Q D, et al. Electronic Circuit Model Construction of A Synthetic Gene Network [J]. Journal of Tianjin University of Science & Technology, 2011.

[5] Javier M. Buldú, et al. Electronic Design of Synthetic Genetic Networks [J]. International Journal of Bifurcation and Chaos, 2014, 17(10):0701927.

[6] Jing Z, Huang J. Bifurcation and chaos in a discrete genetic toggle switch system [J]. Chaos Solitons & Fractals, 2005, 23(3):887-908.

[7] Zhao X, Ouyang Q, Wang H. Designing a stochastic genetic switch by coupling chaos and bistability [J]. Chaos an Interdisciplinary Journal of Nonlinear Science, 2015, 25(11):6917.

[8] Feng L, Xiang Y, Sun F, et al. Bifurcation Analysis and Chaotic Behavior of a Discrete-time Delayed Genetic Oscillator Model [J]. Advances in Difference Equations, 2017, 2017(1):3.

[9] Din Q. Stability Analysis of a Biological Network [J]. Network Biology, 2014, 4(3)

[10] Luís Rafael, Elias R . Local Stability in 3D Discrete Dynamical Systems: Application to a Ricker Competition Model [J]. Discrete Dynamics in Nature and Society, 2017, 2017:1-16.

[11] He Lianghua, Modern Control Theory and Application [M]. Wuhan: China University of Geosciences Press, 2013

[12] Ingalls B P. Mathematical Modeling in Systems Biology: An Introduction [J]. 2014.

[13] Hellen E H, Kurths J, Dana S K. Electronic circuit analog of synthetic genetic networks: Revisited [J]. European Physical Journal Special Topics, 2017, 226(9):1811-1828.

[14] Haustenne L, Bastin G, Coron J M, et al. On stability analysis of genetic regulatory networks represented by delay-differential equations [J]. IFAC-Papers on Line, 2015, 48(1):453-457.

Author details

First Author: School of Automation, China University of Geosciences, Wuhan, 430074, P.R. China.
Songo Higher Education Polytechnic Institute, Tete, 3204, Republic of Mozambique.

Second Author: School of Automation, China University of Geosciences, Wuhan, 430074, P.R. China. E-mail: fliu@cug.edu.cn

ISSN 2250-3153
Correspondence Author: E-mail: felmateus@hotmail.com ,
Tel: +86-15072491782